

# Applications of the Gauge Repeatability and Reproducibility Framework to Complex Data Science Structures

Kiegan Rice

The title is a work in progress. Don't love it yet. I like the title

## Contents

<b>1</b>	<b>Introduction</b>	<b>1</b>
1.1	Complex Data Structures . . . . .	2
1.2	Automated Forensic Firearms Analysis . . . . .	3
<b>2</b>	<b>Methodology</b>	<b>5</b>
2.1	Reframing Gauge R&R for Signature Data . . . . .	8
2.2	Reframing Gauge R&R for Similarity Scores . . . . .	12
<b>3</b>	<b>Data Collection</b>	<b>14</b>
<b>4</b>	<b>Results</b>	<b>15</b>
4.1	LEA signatures . . . . .	15
4.2	Pairwise Similarity Scores . . . . .	16
<b>5</b>	<b>Conclusions</b>	<b>16</b>

## 1 Introduction

Gauge Repeatability and Reproducibility (Gauge R&R) studies are traditionally used in engineering fields as part of measurement systems analysis. Gauge R&R studies focus on measuring the repeatability and reproducibility of a measurement process within and across environmental conditions [Vardeman and VanValkenburg, 1999]. Their study design assumes a univariate measurement value resulting from some measurement process and aims to quantify sources of variability around a single measurement average.

As data collection and analysis become more complex, the Gauge R&R framework must be adapted to allow for a broad definition of measurement data. We focus on adapting the traditional Gauge R&R framework to complex data structures. In the following, we describe the complex nature of modern measurement data and methods for adapting the Gauge R&R framework to quantify measurement repeatability and reproducibility.

Consider the length of a manufactured screw,  $y$ . Suppose the length of that screw  $y$  is measured by multiple operators using multiple tools. In that case a Gauge R&R model can be used to determine to what degree the variability in the set of resulting measurements can be attributed to differences across operators or tools.

Gauge R&R studies utilize a basic random-effects model, assuming one overall measurement mean and a set of random effects corresponding to study design factors, such as operator and measurement device. The quantities of interest are primarily the variance components associated with each random effect, which describe both the overall measurement process variability as well as the degree to which measurement variability is related to each study factor.

There are several useful applications of variance components obtained from a Gauge R&R study. One major outcome is the ability to compare any two objects for similarity. Consider the difference in measured length between two manufactured screws, say  $y_a$  and  $y_b$ :  $y_a - y_b = d$ . We can assess whether the magnitude of  $d$  falls within a reasonable range of measurement variability given previously quantified repeatability and reproducibility components. If the difference in measured length  $d$  falls within an acceptable range, the two objects can be considered quantitatively similar after allowing for variability in measurement.

The length of the screw in our example is a univariate response measurement. Quantifying the similarity of two objects and accounting for measurement variability is more challenging when working with complex data structures.

## 1.1 Complex Data Structures

The birth of data science and significant improvements in computing power have opened up new avenues in measurement systems analysis. Data collection and analyses are much quicker and easier today than ever before. Measurement systems can collect data in greater detail, often taking on complex forms with unique structures.

Consider our example of screw length. We may want to measure multiple characteristics of that screw to more completely capture the object as a whole. To get a sense of whether any two screws are genuinely similar, we can compare more than just a singular characteristic. The problem of comparing the set of screw characteristics measured on any two manufactured screws to determine whether they are sufficiently similar

is then more difficult. Screws are a simple traditional example which naturally applies in engineering fields. However, there are many non-traditional data forms which can be captured using measurement systems, due in part to the growth of data science, a field which often leverages complex data structures.

The field of data science often leverages complex data structures. Data science deals in “pipelines” that begin with complex data structures apply sequential actions such as data processing and data transformation to the data to extract useful information and achieve some quantitative result [Donoho, 2017]. In many applications, the pipeline involves data captured using a measurement system, and there is measurement uncertainty associated with the resulting data.

To leverage complex data structures while taking measurement variability into account, we must adapt the definition of distance between any two objects with complex structure, and carefully consider how we apply statistical models to quantify measurement variability.

There have been several approaches that apply Gauge R&R models to multivariate data. Sweeney [2007] considers two-dimensional response data and accounts for the correlation between the two responses of interest when estimating variance components. Peruchi et al. [2013] proposes a weighted principal components (WPC) approach to multivariate Gauge R&R and compares it with estimates found using MANOVA and traditional principal components analysis (PCA). WPC, MANOVA, and PCA are all applied to data with either four- or five-dimensional response measurements, which each represent a different characteristic of an object of interest.

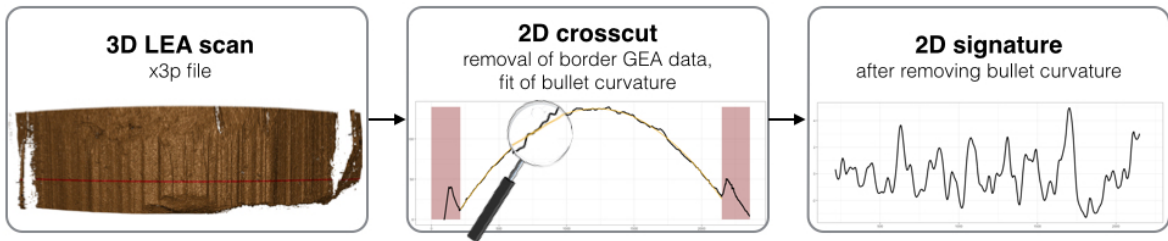
Many data structures utilized in data science include much higher dimensionality than the four- or five-dimensional data used in Peruchi et al. [2013] and the bivariate response in Sweeney [2007]. In addition, there are often structures that inherently differ from traditional multi-dimensional response data. We focus on an application with a more complex structure, and as such, we must consider a different modeling approach.

## 1.2 Automated Forensic Firearms Analysis

We consider the application of data science to automated forensic firearms comparison. When a bullet is fired through a gun barrel, imperfections on lands inside the barrel engrave striation patterns on the bullet’s surface in alternating sections called land engraved areas (LEAs). Striation patterns, which visually appear as a series of peaks and valleys, are the primary evidence used to answer the forensic question of interest: whether two bullets originated from the same source or different sources.

In recent years, researchers have proposed several approaches to automating the comparison of bullet striation patterns using surface topographies of bullet LEAs captured using high-resolution microscopes (De Kinder

**Process 1: Measurement and Data Processing**



**Process 2: Quantifying Object Similarity**

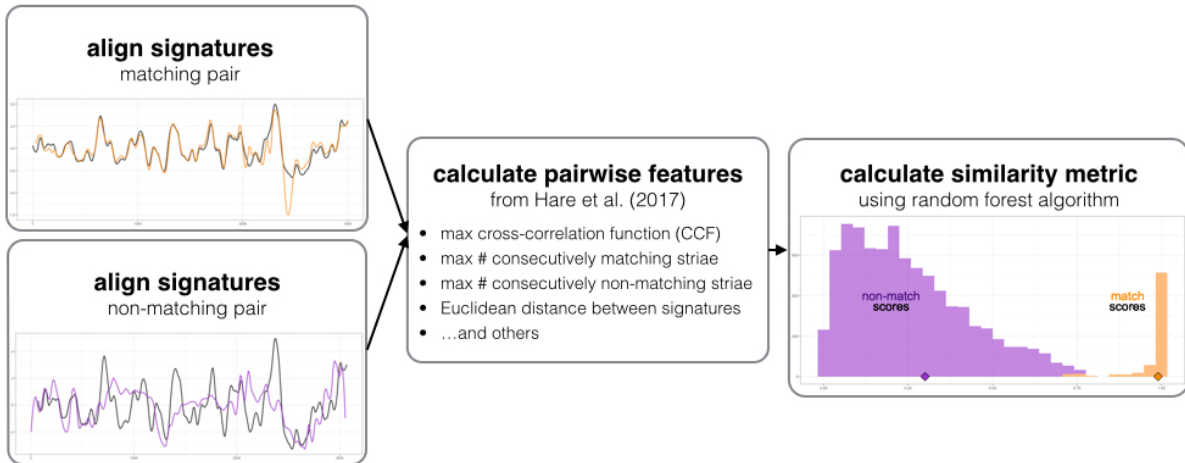


Figure 1: Process of automated firearms comparison as proposed by Hare et al. [2017]. There are two stages of measurement within the full process. First, 3D microscopy is used to capture a three-dimensional surface topography of a bullet LEA. Automated data processing techniques are used to remove bordering GEA data as well as bullet curvature. The result is a two-dimensional LEA signature. The second process involves pairing and aligning two data objects, extracting pairwise features, and calculating a pairwise similarity metric. **One more thing - purely aesthetically - could you vertically center the very last box? :)**

and Bonifanti [1999], Chu et al. [2010], Chu et al. [2013], Hare et al. [2017]). Figure 1 shows an overview of the comparison process proposed by Hare et al. [2017].

Automated bullet comparison uses a data science approach to translate the complex striation pattern on bullet LEAs into measured data and subsequently calculate similarity metrics for any two bullet LEA striation patterns. Two LEA patterns originating from the same source (the same land in the same barrel) should have a high similarity score, while two LEA patterns from different sources should receive a low similarity score.

The data pipeline developed by Hare et al. [2017] relies on the high-resolution microscopy measurement system. It is essential to establish the repeatability and reproducibility of the data capture and successive similarity analysis. However, the complex nature of striation patterns does not naturally lend itself to the traditional Gauge R&R framework for univariate measurement data.

This paper presents two adaptations to the Gauge R&R framework as they apply to two distinct data structures within the data science pipeline of forensic firearms analysis. We use automated analysis methods as a motivating example for the two approaches described hence.

The structure of this paper is as follows: we first present the general three-factor Gauge R&R model and its assumptions in Section 2, then describe two forensic firearms analysis data structures in detail and propose meaningful adaptations to the Gauge R&R framework to best leverage repeated measurement data (Sections 2.1, 2.2). We then outline the scope of data collected in our study (Section 3), show results from both model frameworks (Section 4), and discuss the implications of our work (Section 5).

## 2 Methodology

I was tripped up by this in your defense, and I am again being tripped up in the paper by having the traditional model explained first and then changed later. I believe I have figured out why - I've explained it in section 2.1

The traditional three-factor gauge R&R model is defined as follows: for parts  $p_j : j = 1, \dots, n_p$ , operators  $o_k : o = 1, \dots, n_o$ , devices  $d_m : m = 1, \dots, n_d$ , and repetitions  $r_n : n = 1, \dots, n_r$ , let  $y_{jkmn}$  be the measured response value for part  $j$ , operator  $k$ , device  $m$ , and repetition  $n$ . Define a mixed-effects model,

$$y_{jkmn} = \mu + p_j + o_k + d_m + po_{jk} + pd_{jm} + od_{km} + pod_{jkm} + \epsilon_{jkmn}, \quad (1)$$

where  $\mu$  is a fixed, unknown measurement mean and all other model components are random effects

[Montgomery and Rungger, 1993]. Assume all effects  $p_j$ ,  $o_k$ ,  $d_m$ ,  $po_{jk}$ ,  $pd_{jm}$ ,  $od_{km}$ , and  $pod_{jkm}$  are independent and identically distributed random variables which follow normal distributions centered at zero but have different variances. To clarify the connection between an effect and its variance, we index a variance by its corresponding effect; for example,  $p_j \stackrel{iid}{\sim} N(0, \sigma_p^2)$ . We also assume  $\epsilon_{jkmn} \stackrel{iid}{\sim} N(0, \sigma^2)$ .

Of primary importance in measurement systems analysis are the estimates of variance components associated with each random effect. For example, the estimated value of  $\sigma_d^2$ ,  $\hat{\sigma}_d^2$ , estimates the variance in the measurement process associated with differences across measurement devices. We also consider two summary values: We report these sigams in a table at the end, but how about shortening to "repeat" and "reprod" as text, as below? can update table too if we like this. XXX much better!

$$\sigma_{\text{repeat}} = \sqrt{\sigma^2} \quad \text{and} \quad (2)$$

$$\sigma_{\text{reprod}} = \sqrt{\sigma_o^2 + \sigma_d^2 + \sigma_{po}^2 + \sigma_{pd}^2 + \sigma_{od}^2 + \sigma_{pod}^2}. \quad (3)$$

$\sigma_{\text{repeat}}$  estimates variability of measurements taken under the same environmental conditions, while  $\sigma_{\text{reprod}}$  estimates variability of measurements across differing environmental conditions.

To adapt this traditional three-factor model to our firearms analysis data pipeline, we must carefully consider the structure of our data. We discuss the structure of our data and ensuing adaptations in detail in sections 2.1 and 2.2.

Automated forensic firearms analysis utilizes data to answer the forensic question of whether two bullets were fired through the same gun barrel. We distinguish between same-source or different-source origin for any two bullets by measuring the degree of similarity between them. Within the automated analysis pipeline, this is achieved with two stages of measurement. Both are depicted in Figure 1. The first measurement process involves capturing the surface topography of bullet LEAs and extracting a two-dimensional “signature” capturing the striation patterns engraved by the gun barrel. The second measurement process deals with pairs of signatures by extracting pairwise features and subsequently calculating a pairwise similarity metric. Both measurement processes result in data structures too complex for the scope of the traditional Gauge R&R model defined in Equation 1.

Measurement process 1 translates a physical object – the surface of a bullet LEA – to a complex data structure. Trained microscope operators stage bullets in high-resolution microscopes to capture relative height values on a regular grid. The result is an x3p (XML 3-D Surface Profile) file that contains a matrix of height

measurements  $\mathbf{Z} = z_{i,q}$  where  $i = 1, \dots, n_x$  and  $q = 1, \dots, n_y$ . The pattern of interest on the bullet surface is the striation pattern, a series of peaks and valleys corresponding to scratches engraved by micro-imperfections in the gun barrel.

We extract the striation pattern using the two-step procedure proposed in Hare et al. [2017], shown in Figure 1. First, we identify an optimal cross-section height,  $y_{opt}$ , and calculate a bullet profile by aggregating height measurements along a small band (marked in light red) across the bullet surface. The resulting height measurement is denoted as  $z_i$  for each location  $i$  along  $x$ . Note that  $z_i$  is really an average, i.e.  $\bar{z}_i$ . We adopt the simpler notation for the sake of clarity in presenting results. To counter effects from the structurally different neighboring groove engraved areas (GEAs) we remove data from these regions, model and remove bullet curvature. This process results in a LEA “signature” capturing the striation pattern of peaks and valleys as deviations from global bullet structure. For additional details on signature extraction, see Hare et al. [2017] and Rice et al. [2020].

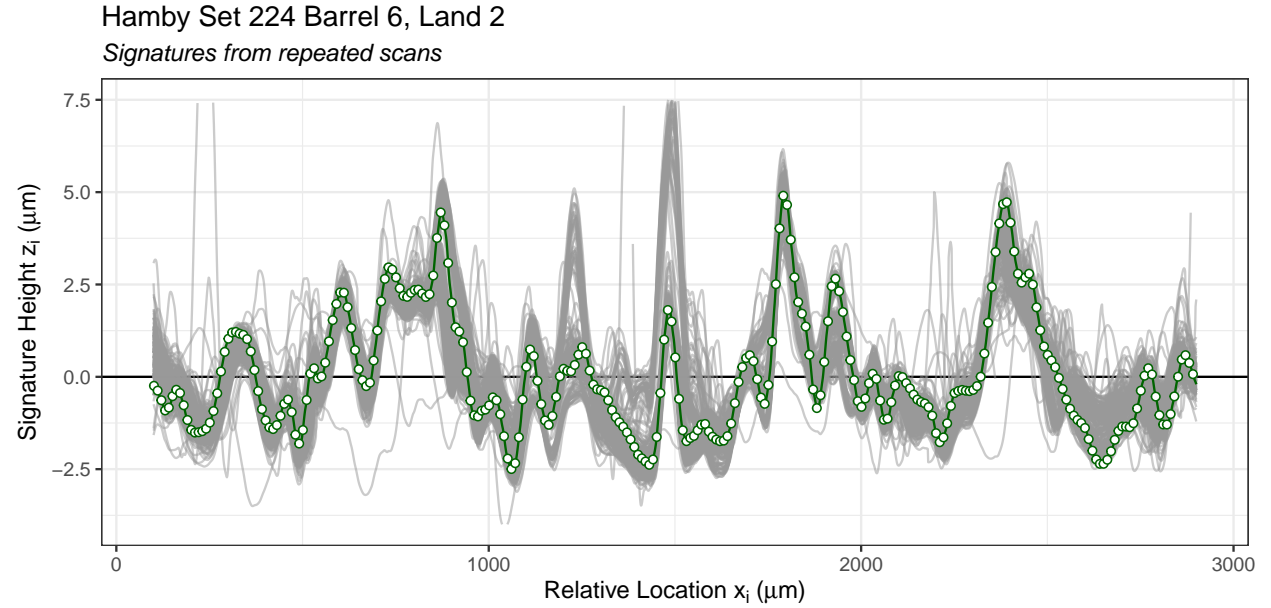


Figure 2: Two-dimensional signature data utilized in automated forensic firearms analysis. A total of 228 signatures corresponding to scans of land 2 in barrel 6 of the Hamby set 224 are shown. One of the signatures is emphasized as green line, every 10<sup>th</sup> data point is drawn. The data structure consists of equidistant  $x_i$  locations with corresponding relative height values  $z_i$ . Most signatures contain several missing  $z_i$  values.

The resulting LEA signatures are a sequence of residual values  $e_i = z_i - \hat{z}_i$ , where  $\hat{z}_i$  are predicted height values for location  $x_i$  from a LOESS model fit to the bullet curvature. The series of relative height measurements and their corresponding locations  $x_i$  are the structure of interest, so for clarity we will denote LEA signatures as a set of measurements  $(x_i, z_i)$ ,  $i = 1, \dots, \ell$  where  $\ell$  is the number of  $x$  locations on a signature for LEA  $L$ . Figure 2 depicts 228 signatures corresponding to scans from three bullets of barrel 6 in Hamby set 224.

Scans were taken by multiple operators on two different microscopes. These repetitions are shown in grey, and demonstrate the variability within the measurement process of translating striation patterns on bullets to signature data objects. One of these signature is singled out and shown in dark green to emphasize the general structure. The signatures depicted in Figure 2 have been aligned in  $x$  direction using maximum cross-correlation function. In addition, trailing edges of each signature were trimmed to balance  $x$  location indices for modeling.

Measurement process 2 deals with answering the forensic question: were two bullets fired from the same gun barrel? The forensic question is addressed at the LEA level. By comparing pairs of LEAs from two bullets we determine whether any of the LEA striation patterns match based on a similarity metric which aims to separate “matching” LEA pairs from “non-matching” LEA pairs. In the data pipeline suggested by Hare et al. [2017] a set of pairwise features is extracted from aligned signatures, such as the cross-correlation function, the number of consecutively matching striae, and the number of non-matching striae. These features provide information about the level of similarity between any two objects. This set of paired features is used in a random forest model trained in Hare et al. [2017] to predict a similarity score for each pair of signatures with possible values in  $[0, 1]$ . The pairwise nature of the comparisons introduces complexity to measurement analysis; modeling variability in relation to environmental conditions requires a redefinition of the framework traditionally used to consider environmental conditions in Gauge R&R.

We next propose adaptations to the traditional Gauge R&R framework that accommodate the complex data structures resulting from both Measurement Process 1 and 2: LEA signature data and the pairwise similarity score.

## 2.1 Reframing Gauge R&R for Signature Data

The structure of LEA signature data introduces two primary obstacles to utilizing the traditional Gauge R&R framework. First, the measured response is composed of a set of structured measurements rather than a single value. Secondly, the structure of peaks and valleys in LEA signatures violates an assumption of independence for measured response values. To address these incongruities, we have to make two modifications to the traditional three-factor Gauge R&R model. The first adaptation focuses on the model’s fixed effect structure, while the second focuses on data reduction for compliance with independence assumptions.

We define a model to estimate measurement variability of LEA signatures in the following way. Let  $z_{Lijkmn}$  be the measured signature height value for land  $L = 1, \dots, 6$  at location  $x_i : i = 1, 2, \dots, \ell$ , on part  $j$ , scanned by operator  $k$ , on device  $m$ , and at repetition  $n$ .

$$z_{Lijkmn} = \mu_{Li} + p_{Lij} + o_{Lik} + d_{Lim} + po_{Lijk} + pd_{Lijm} + od_{Likm} + pod_{Lijkm} + \epsilon_{Lijkmn}, \quad (4)$$

where  $\mu_{Li}$  is a fixed, unknown measurement average by location index  $i$  on land  $L$ , and all other model components are random effects. Assume each  $p_{Lij}$ ,  $o_{Lik}$ ,  $d_{Lim}$ ,  $po_{Lijk}$ ,  $pd_{Lijm}$ ,  $od_{Likm}$ , and  $pod_{Lijkm}$  are independent and identically distributed random variables which follow normal distributions centered at zero and have respective differing variances; for example,  $p_{Lij} \stackrel{iid}{\sim} N(0, \sigma_p^2)$ . Also assume  $\epsilon_{Lijkmn} \stackrel{iid}{\sim} N(0, \sigma^2)$ .

Note that Equation 4 contains a more complex fixed effect structure than the traditional model defined in Equation 1. We define a fixed effect  $\mu_{Li}$  indexed by both land  $L$  and location  $i$  in order to separate structural variability in the signature from measurement variability, the mechanism of interest. LEA signature data contain an inherently complex structure of center, as signatures consist of a series of peaks and valleys which act as the signal of interest for evidence comparison. We are interested in measuring the variability around that signal measurement rather than variability of the signal itself, and therefore must account for differences in structural height by location as part of the fixed effects structure.

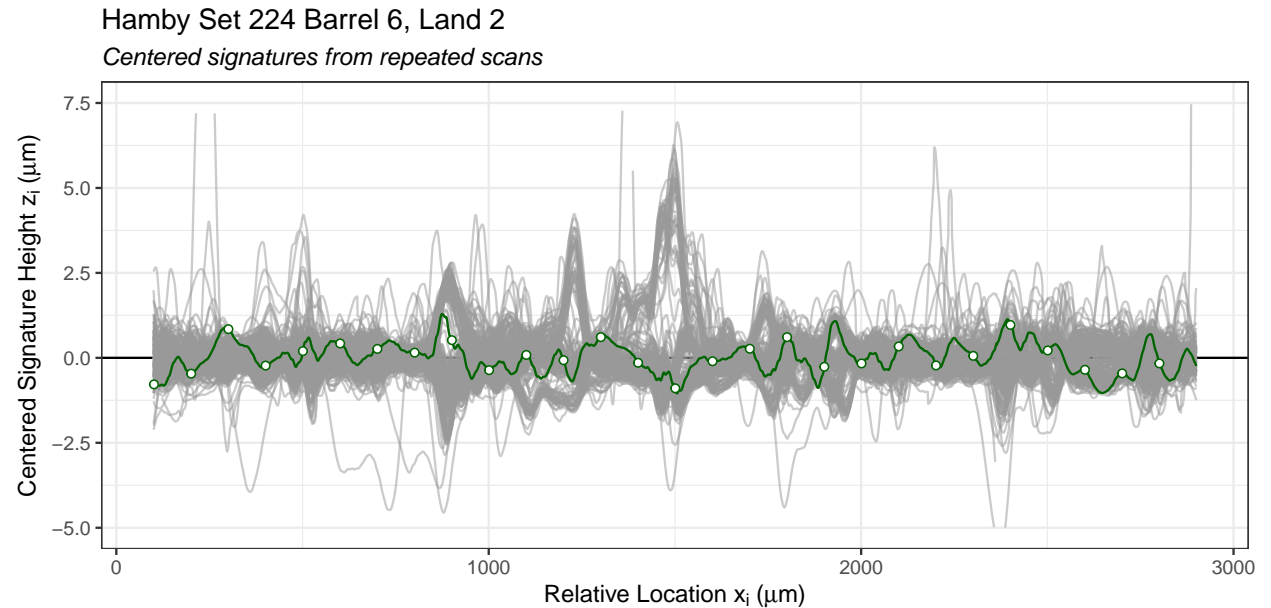


Figure 3: Two-dimensional signature data, centered by subtracting the mean in each location  $x_i$ . One exemplar centered signature is shown in green, with points emphasized at each 100<sup>th</sup>  $x_i$  location.

XXX this will go away XXXThe three-factor model defined in Equation 1 defines all effects as random save for a single fixed effect: a fixed, measurement average,  $\mu$ . LEA signature data inherently contain a more complex structure of center, as signatures are not made up of a univariate response corresponding to a single measurement value. XXX Rather than motivating the location based means as mis-characterization of the

variability, let's frame it as a separation of signal and variability: the fixed effects give us the structure of the signal that is being measured, i.e the mean signature of the barrel land as engraved on multiple bullets (which we are usually interested in during the comparison process). The variability around the mean is of interest now, because we can characterize different sources of variability this way. Failing to account for differences in structural height by location will result in mischaracterization of variance components within the model; variability estimates will include the object's structural variability rather than measurement variability. To address this, we define the model's fixed effect structure by location  $x_i$  on each land  $L$ :  $\mu_{Li}$ .

The practical implication of including a fixed effect by location in the model is demonstrated in Figure 3. After centering signature height values by the mean height measurement from all repetitions at location  $x_i$ , remaining variability around the center is greatly reduced, and more adeptly captures measurement variability rather than structural variability.

XXX which structure are you addressing here? grouping structure is a term from programming. It should be rephrased as random structure. However, I am not completely sure which random effects you are referring to.

Despite this adjustment, there is still significant structure remaining in the LEA signature data which may lead to systematic underestimation of quantities of interest when left in the model, such as the variance components associated with operator and device. The approach to mitigating this misrepresentation, is to carefully define the grouping structure used to estimate variance components. We define random effect grouping structure by both study factor and location  $Li$ , practically accomplished by interacting location with study factor in each random effect. Consider for example the variability of measurements across devices. It is of interest whether one device captures more extreme values, such as higher peak measurements and lower valley measurements. XXX the next sentence is very hypothetical. If we defined a random effect for device and grouped by device alone, without accounting for structural differences by location, extreme highs and extreme lows would average out across the entire group and the variability would be artificially deflated. XXX I like the new structure XXXThis will go away: We address this by defining the random effect groups by both study factor and location  $Li$ . This is accomplished by interacting location with study factor in a random effect.

Adaptations to the fixed effect and grouping structure ensure that the estimated variance components associated with the model accurately represent quantities of interest. However, the independence assumption for response values is violated and needs to be addressed before a random effects model can be properly applied to the LEA signature data structure.

Estimating covariance matrices for signature data and incorporating data covariance into the model would be

computationally intensive and extremely complex XXX we don't know that it's unnecessary for answering questions of repeatability and reproducibility in bullet LEA data. We therefore focus on a different approach. To uphold the traditional model structure and satisfy the independence assumption, we propose to break dependencies by subsampling the data at equidistant  $x_i$  locations. The result is then a set of measurements of the form:

$$(x_i, z_i) : i = 1, 1 + w, 1 + 2w, \dots, 1 + cw \quad (5)$$

where  $w \in \mathbb{N}$  is some subsampling window size, with positive integer  $c$  such that  $1 + cw < \ell$ , where  $\ell$  is the maximum index  $i$  for  $x_i$  locations for signatures from land  $L$ . The necessary window between sampling locations,  $w$ , differs based on application and data structure. Here, we propose a window of  $w = 100$  based on typically observed autocorrelation (ACFs) in signature data as shown in Figure 4. Because of large auto-correlation in successive striae, we see that the structure in signature data is not a traditional dependence data structure, such as time series or spatial data, with monotonic decrease of dependence with increase in lag. XXX the next sentence reads a bit like an after thought - you might want to get rid of the 'also' and the ', and'. We also completed a sensitivity analysis for window size  $w$ , and on average estimated variance components remained consistent for window sizes between  $w = 10$  and  $w = 150$ .

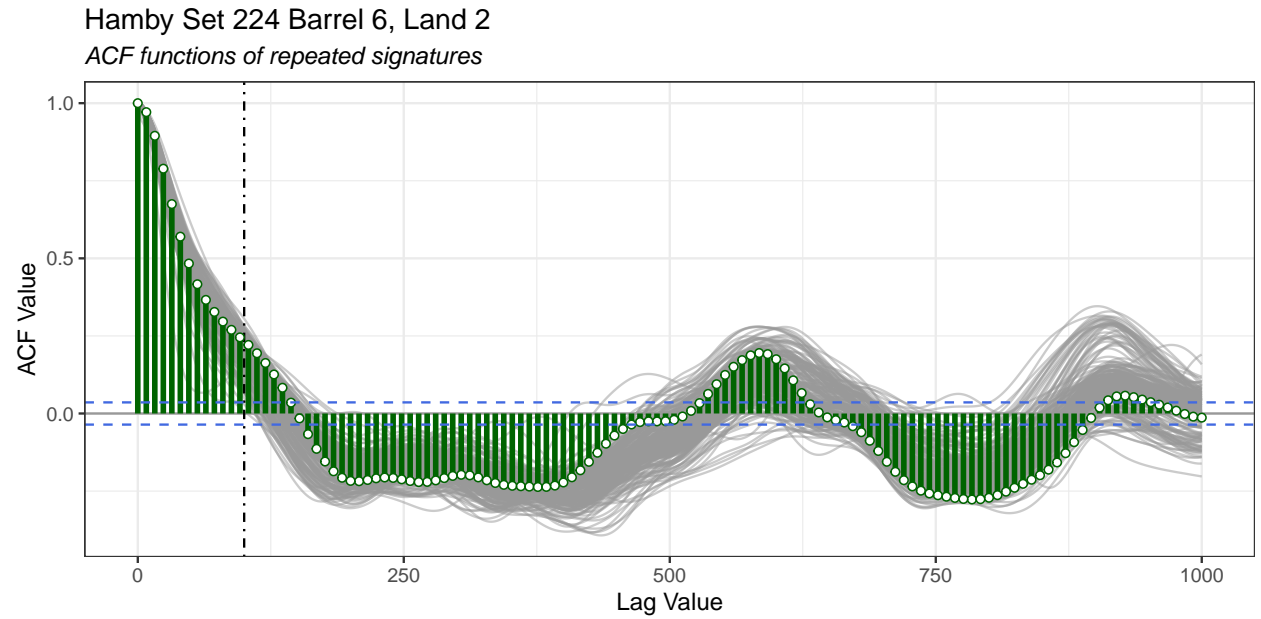


Figure 4: Autocorrelation functions (ACFs) for each repeated signature of Barrel 6, Land 2, shown for lags between 0 and 1000. One exemplar ACF is shown in green in the foreground. Autocorrelation drops off significantly for the signature structure by lag 100. The exemplar ACF crosses zero near lag 150. When considering all six lands in the barrel, the ACF is typically low by lag 100.

The model is used as stated in Equation 4, but using data at subsampled indices  $x_i : i = 1, 101, \dots, 1 + 100 * c$ .  
 XXX XXX I agree, you introduced it nicely above the rest of this can go away if we like the new framing:  
 The resulting model we use to estimate measurement variability of LEA signatures is then as follows. Let  $z_{Lijkmn}$  be the measured signature height value for land  $L = 1, \dots, 6$  at location  $x_i : i = 1, 101, \dots, 1 + 100 * c$ , on part  $j$ , scanned by operator  $k$ , on device  $m$ , and at repetition  $n$ .

$$z_{Lijkmn} = \mu_{Li} + p_{Lij} + o_{Lik} + d_{Lim} + po_{Lijk} + pd_{Lijm} + od_{Likm} + pod_{Lijkm} + \epsilon_{Lijkmn}, \quad (6)$$

where  $\mu_{Li}$  is a fixed, unknown measurement average by location index  $i$  on land  $L$ , and all other model components are random effects. Assume each  $p_{Lij}$ ,  $o_{Lik}$ ,  $d_{Lim}$ ,  $po_{Lijk}$ ,  $pd_{Lijm}$ ,  $od_{Likm}$ , and  $pod_{Lijkm}$  are independent and identically distributed random variables which follow normal distributions centered at zero and have respective differing variances; for example,  $p_{Lij} \stackrel{iid}{\sim} N(0, \sigma_p^2)$ . Also assume  $\epsilon_{Lijkmn} \stackrel{iid}{\sim} N(0, \sigma^2)$ .

One additional aspect to consider is the significant reduction in data caused by the subsampling scheme. To address this concern, we fit a series of phased models for each set of repeated signatures which use data subsampled using the same window size  $w$ , but whose starting index is staggered throughout the width of a single window. To fit ten phased models with a window size  $w = 100$ , we stagger the starting index at each  $10^{th}$  location:

$$\begin{aligned} \text{Phase 1: } & 1, 101, \dots, 1 + 100 * c \\ \text{Phase 2: } & 11, 111, \dots, 11 + 100 * c \\ & \vdots \quad \vdots \\ \text{Phase 10: } & 91, 191, \dots, 91 + 100 * c. \end{aligned} \quad (7)$$

The phased approach incorporates a larger proportion of the original data points, and with ten individual estimates for each variance component, provides a range of uncertainty for the estimates while still satisfying the independence assumption needed for each individual model. The combination of subsampling and phased models helps achieve a balance between over-downsampling and reducing dependency.

We next consider the second data format in the Hare et al. [2017] data pipeline.

## 2.2 Reframing Gauge R&R for Similarity Scores

The structure of pairwise similarity scores presents a different obstacle to the Gauge R&R framework from the LEA signatures. Similarity scores from Measurement Process 2 are univariate, singular measurement values without the challenge to independence that LEA signatures present. However, the levels of study factors parts, operators, and devices no longer have a one-to-one relationship with the levels of study factors represented in a single response measurement. Beyond that, specifying a singular measurement average  $\mu$  as the fixed effects structure ??as done in]model1 does not fully capture the mean structure.

We first consider the problem of paired study factors. When any two pairs of measured LEA signatures are compared, the signatures have been collected either under the same or under two differing sets of environmental conditions. For example, two same-source LEA signatures may have been scanned on the same machine, but by different operators. **This phenomenon has to be addressed when** considering the response value,  $z$ .

**We are primarily interested** in variance components associated with differing environmental conditions. In order to determine whether the pairwise measurement process is reproducible across measurement conditions, we investigate variability of pairwise scores resulting from scans in a variety of environmental conditions. To capture this mechanism, we consider each possible pair of environmental conditions as a grouping, i.e instead of considering whether the object was measured by Operator A, B, or C, we consider the pair of operators represented in the pairwise score: Operator A and Operator A (A-A), Operator A and Operator B (A-B), Operator A and Operator C (A-C), et cetera. This grouping structure provides the closest parallel to traditional R&R grouping structure: all pairs of environmental conditions are represented as groups, and we measure variability of resulting scores across those groups. We can then estimate how much of the variability in pairwise scores can be attributed to differences between any pair of operators. If one operator has scans that differ from other operators, that mechanism will be captured in their pairings with each of the other operators.

We therefore re-index the response data in the following way. Let  $z_{(L)(j)(k)(m)(n)}$  be the pairwise similarity score resulting from Measurement Process 2 for land pairing  $(L) : 1 - 1, 1 - 2, \dots, 6 - 6$ , part pairing  $(j) : 1 - 1, 1 - 2, \dots, 3 - 3$ , operator pairing  $(k) : A - A, A - B, \dots, G - H, H - H$ , device pairing  $(m) : 1 - 1, 1 - 2, 2 - 2$ , and repetition pairing  $(n) : 1 - 1, 1 - 2, \dots, 5 - 5$ . The updated indexing addresses the first modeling concern.

The second adaptation to the Gauge R&R framework redefines the fixed effects. When considering pairwise scores from pairs of lands,  $(L) : 1 - 1, 1 - 2, \dots, 6 - 6$ , we must account for the nature of the similarity metric. As shown in Figure 1, similarity scores for matching pairs fall within a small spread towards the top of the

range, while non-matching pairs have a much more diffuse distribution which falls to the middle and lower end of the range. XXX where did you get the distribution from? Usually we see the opposite in terms of the variability for the densities. We expect matched pairings  $(1 - 1, 2 - 2, \dots, 6 - 6)$  to have similar mean structures; however, we do not expect the same property of the non-matching pairings. Non-matching pairs are not necessarily different *in the same way*. That is, scores for the pairing  $1 - 2$  may be very low and close to 0.1, whereas scores for the pairing  $1 - 4$  may be higher and fall near 0.4. For this reason, we consider the land-to-land pairing index to be a critical component of the fixed effects structure. We expect scores for each land-to-land pairing to vary around a common mean  $\mu_{(L)}$ , and aim to measure that variability.

The spread of scores also differs by land pairing: non-matching land pairs have more diffuse distributions, and some land-to-land pairs may have more or less diffuse score distributions than others by nature. To account for these distributional differences, we also interact land pairing index with the random effect grouping structures to ensure we fully capture variability due to environmental conditions. The resulting model for pairwise scores is then:

$$\begin{aligned} z_{(L)(j)(k)(m)(n)} = & \mu_{(L)} + p_{(L)(j)} + o_{(L)(k)} + d_{(L)(m)} + po_{(L)(j)(k)} + pd_{(L)(j)(m)} + od_{(L)(k)(m)} \\ & + pod_{(L)(j)(k)(m)} + \epsilon_{(L)(j)(k)(m)(n)}, \end{aligned} \quad (8)$$

We next describe the scope of data collected, present results from modeling both LEA signature data and pairwise similarity scores, and discuss conclusions reached from adapting the modeling framework.

### 3 Data Collection

The data collected for this study were x3p (XML 3-D Surface Profile) data objects capturing the surface topography of bullet LEAs. The resulting data structures, as described previously, are two-dimensional LEA signatures resulting from data processing during Measurement Process 1, and pairwise similarity scores for pairs of LEA signatures resulting from Measurement Process 2. We next describe the scale of the study and environmental conditions.

XXX Study design is the only subsection. You are also mentioning environmental conditions - should that be another subsection? If not, I'd suggest to get rid of the study design header. The section is short enough that it doesn't need that additional structure. done! we can talk more about environmental conditions, but it's less important for the focus of this paper.

The Gauge R&R study focused on varying three environmental conditions: parts, devices, and operators. In the study, parts are considered to be bullets of origin. We focus on three bullets originating from the same Ruger P-85 gun barrel. The bullets, which originate from Hamby set 224, were physically fired and collected as part of a large-scale study on accuracy of firearms examination conclusions [Hamby et al., 2009]. Each bullet contains six LEAs, each engraved by contact with one of the six lands inside the same gun barrel.

XXX mention damage to bullet and maybe show in a picture what you mean by it.

Each LEA was scanned on two devices by eight operators at least three times. Each operator was tasked with collecting between three and five repeated scans of each bullet on each device (high-resolution microscope), spread out over time as a series of “Rounds”. A single round consisted of a capture of each LEA on each bullet once on Microscope 1 and once on Microscope 2. Operators were directed to complete each round in its entirety before moving on to the next round. Seven operators completed five rounds, while one operator completed three rounds. This collection scheme resulted in a total of 228 repeated captures of each of the six LEA signatures, with 1368 LEA signatures in total.

While the three bullets originate from the same barrel, pairwise comparisons are completed at the land-to-land level, resulting in a set of pairwise comparisons which represent a mix of same-source and different-source pairs. For example, each LEA on Bullet 1 only originates from the same source (here land) as one of the six LEAs on Bullet 2. All other comparisons are considered different-source pairs. The result is over 930,000 paired comparisons, with over 100,000 same-source comparisons and over 700,000 different-source comparisons.

XXX How does this break down look like when you consider damaged lands?

## 4 Results

Within the collected data, there were several LEAs with surface damage. In forensic science practice, firearms examiners deem LEAs with damage unsuitable for comparison and they are removed from consideration. Under each model, we fit models which include all available data as well as a set of models which removed all signatures originating from damaged LEAs. Both sets of results are reported for both LEA signatures and pairwise scores.

Models were fit using the `lmer()` function in the `lme4` package in R, and Restricted Maximum Likelihood (REML) was used for parameter optimization.

## 4.1 LEA signatures

Variance components were estimated for each individual land  $L$  as well as for a set of data pooled across all six lands  $L = 1, \dots, 6$ . The model in Equation 4 was used for all seven sets of estimates, with land index  $L$  held constant for models on each individual land. Ten phased models were fit for each data set with window size  $w = 100$ . Results are reported in Table 1 by variance component as **average, minimum, and maximum** estimate per component across the ten phased models. Results are also summarized visually in [the boxplots of Figure 5](#).

The variance components with the largest magnitude are those associated with parts and residual error. In the study, parts are bullets of origin. This result is not surprising, due to the fact that striation patterns contain some amount of structural variability originating from the engraving process, as opposed to measurement variability due to differences in operators or microscopes.

[XXX This is the first time you are mentioning damage to the bullets. This needs some additional explanation, see comments above.](#)

Removing damaged LEAs from consideration reduced the magnitude of estimated variance components, most noticeably for the part (bullet) effect and residual error, though a noticeable difference is also seen for the part-operator interaction.

Summary values  $\sigma_{\text{repeat}}$  and  $\sigma_{\text{reprod}}$ , reported in Table 2, demonstrate the same behavior, with models having lower summary values when damaged LEA data is removed. The value of  $\sigma_{\text{reprod}}$  is lower in magnitude than that of  $\sigma_{\text{repeat}}$  for all six lands and the pooled model, which indicates systematic differences in environmental condition (operator and device) contribute less to overall measurement variability than that of inherent measurement error or variability in how the same striation patterns are engraved across different bullets.

## 4.2 Pairwise Similarity Scores

Three models were fit using different sets of data. Similarity scores for all same-source pairs were included in one model, with a second model fit for scores from all different-source pairs. A model which pooled all scores regardless of origin was also fit. Results from these three sets of models are reported in Table 3.

We observe the largest variance components associated with residual error and part (bullet), with other variance components having much smaller magnitude. We also observe that after excluding pairs that include a damaged LEA, the magnitude of the estimated variance components decreases. Summary values,  $\sigma_{\text{repeat}}$  and  $\sigma_{\text{reprod}}$ , are also reported in Table 4. The magnitude of the summary values lessen when damaged LEAs are removed, but not as drastically as the reduction seen in the signature modeling results.

Table 1: LEA signature R&R model estimates for variance components using the model defined in Equation 5. Mean estimate from 10 phased models (min estimate, max estimate).

Land	$\sigma_p$	$\sigma_o$	$\sigma_d$	$\sigma_{po}$
<b>1</b>	0.51 (0.46, 0.57)	0.07 (0.06, 0.08)	0.04 (0.00, 0.06)	0.14 (0.12, 0.17)
<i>damage excluded</i>	0.24 (0.20, 0.30)	0.08 (0.07, 0.10)	0.09 (0.07, 0.11)	0.09 (0.05, 0.13)
<b>2</b>	0.44 (0.32, 0.55)	0.08 (0.05, 0.11)	0.08 (0.08, 0.09)	0.04 (0.00, 0.08)
<b>3</b>	0.55 (0.44, 0.62)	0.00 (0.00, 0.02)	0.08 (0.07, 0.10)	0.13 (0.11, 0.15)
<b>4</b>	0.80 (0.65, 0.98)	0.00 (0.00, 0.03)	0.03 (0.00, 0.06)	0.18 (0.16, 0.20)
<i>damage excluded</i>	0.16 (0.12, 0.19)	0.06 (0.06, 0.08)	0.05 (0.03, 0.07)	0.10 (0.07, 0.11)
<b>5</b>	0.45 (0.38, 0.53)	0.06 (0.00, 0.08)	0.06 (0.03, 0.07)	0.27 (0.23, 0.44)
<b>6</b>	1.30 (1.27, 1.36)	0.20 (0.09, 0.28)	0.05 (0.00, 0.10)	0.38 (0.32, 0.44)
<i>damage excluded</i>	0.33 (0.15, 0.46)	0.05 (0.00, 0.11)	0.03 (0.00, 0.06)	0.04 (0.00, 0.10)
<b>Pooled</b>	0.70 (0.66, 0.74)	0.09 (0.00, 0.06)	0.05 (0.00, 0.10)	0.21 (0.20, 0.24)
<i>damage excluded</i>	0.44 (0.37, 0.51)	0.06 (0.05, 0.07)	0.08 (0.07, 0.08)	0.16 (0.14, 0.17)

Land	$\sigma_{pd}$	$\sigma_{od}$	$\sigma_{pod}$	$\sigma$
<b>1</b>	0.07 (0.00, 0.10)	0.03 (0.00, 0.05)	0.00 (0.00, 0.00)	0.53 (0.52, 0.54)
<i>damage excluded</i>	0.04 (0.03, 0.04)	0.04 (0.03, 0.06)	0.01 (0.00, 0.05)	0.32 (0.29, 0.34)
<b>2</b>	0.00 (0.00, 0.00)	0.02 (0.00, 0.06)	0.06 (0.00, 0.09)	0.55 (0.52, 0.59)
<b>3</b>	0.04 (0.03, 0.09)	0.02 (0.00, 0.04)	0.02 (0.00, 0.05)	0.42 (0.39, 0.46)
<b>4</b>	0.04 (0.00, 0.09)	0.02 (0.00, 0.10)	0.14 (0.08, 0.18)	0.59 (0.56, 0.61)
<i>damage excluded</i>	0.01 (0.00, 0.02)	0.07 (0.06, 0.09)	0.01 (0.00, 0.05)	0.39 (0.35, 0.44)
<b>5</b>	0.00 (0.00, 0.00)	0.00 (0.00, 0.00)	0.00 (0.00, 0.00)	0.61 (0.51, 0.76)
<b>6</b>	0.03 (0.00, 0.05)	0.04 (0.00, 0.19)	0.00 (0.00, 0.00)	1.92 (1.90, 1.95)
<i>damage excluded</i>	0.02 (0.00, 0.05)	0.01 (0.00, 0.04)	0.01 (0.00, 0.04)	0.27 (0.33, 0.42)
<b>Pooled</b>	0.02 (0.00, 0.05)	0.01 (0.00, 0.06)	0.00 (0.00, 0.00)	0.87 (0.86, 0.88)
<i>damage excluded</i>	0.00 (0.00, 0.11)	0.00 (0.00, 0.03)	0.00 (0.00, 0.02)	0.48 (0.46, 0.52)

Table 2: LEA signature R&R model estimates for summary quantities,  $\sigma_{\text{repeat}}$  and  $\sigma_{\text{reprod}}$ .

Land	$\sigma_{\text{repeat}}$	$\sigma_{\text{reprod}}$
<b>1</b>	0.53	0.18
<i>damage excluded</i>	0.32	0.16
<b>2</b>	0.55	0.14
<b>3</b>	0.42	0.16
<b>4</b>	0.59	0.23
<i>damage excluded</i>	0.39	0.15
<b>5</b>	0.61	0.28
<b>6</b>	1.92	0.43
<i>damage excluded</i>	0.37	0.08
<b>Pooled</b>	0.87	0.245
<i>damage excluded</i>	0.48	0.18

LEA Signature Model Parameter Estimates, with and without damaged LEAs  
window size = 100, phases = 10

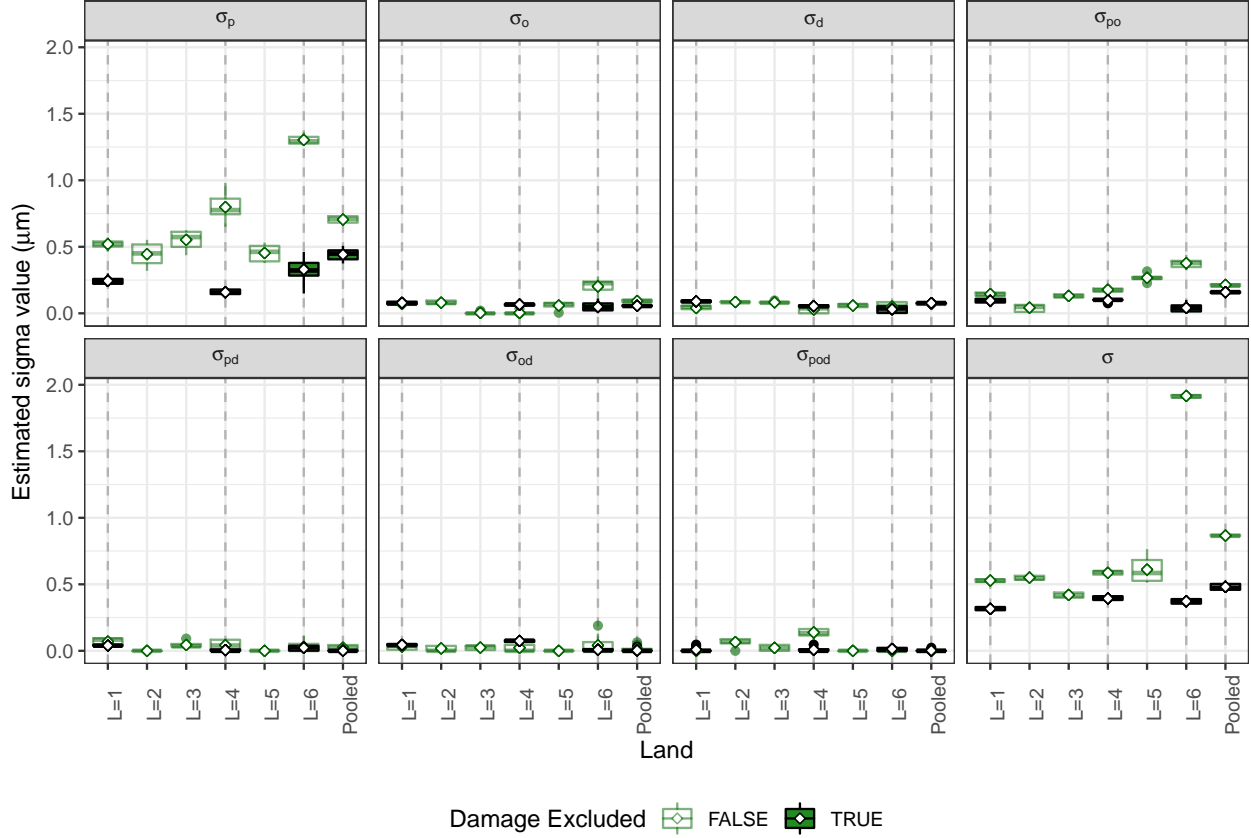


Figure 5: Distribution of variance component estimates resulting from ten phased models applied individually to each of six lands and pooled signature data. Results presented here were modeled using Equation 5. Estimates emphasized in dark green represent estimates after removing damaged LEAs from consideration. **What are the vertical lines?**

Table 3: Pairwise score R&R model estimates for variance components, reported with 95% bootstrap confidence intervals.

Model	$\sigma_{(p)}$	$\sigma_{(o)}$	$\sigma_{(d)}$	$\sigma_{(po)}$
Same-Source	0.212 (0.154, 0.272)	0.027 (0.022, 0.032)	0.020 (0.011, 0.027)	0.050 (0.047, 0.052)
<i>damage excluded</i>	0.067 (0.045, 0.088)	0.030 (0.025, 0.036)	0.023 (0.013, 0.034)	0.042 (0.039, 0.045)
Different-Source	0.035 (0.029, 0.040)	0.011 (0.010, 0.012)	0.003 (0.000, 0.005)	0.016 (0.015, 0.016)
<i>damage excluded</i>	0.034 (0.027, 0.041)	0.010 (0.008, 0.011)	0.000 (0.000, 0.003)	0.015 (0.014, 0.016)
All Pairings	0.117 (0.101, 0.133)	0.017 (0.016, 0.019)	0.011 (0.008, 0.014)	0.029 (0.028, 0.030)
<i>damage excluded</i>	0.045 (0.038, 0.054)	0.018 (0.016, 0.019)	0.011 (0.009, 0.015)	0.025 (0.025, 0.026)

Model	$\sigma_{(pd)}$	$\sigma_{(od)}$	$\sigma_{(pod)}$	$\sigma$
Same Source	0.013 (0.011, 0.016)	0.022 (0.020, 0.024)	0.003 (0.000, 0.007)	0.159 (0.159, 0.160)
<i>damage excluded</i>	0.009 (0.006, 0.012)	0.029 (0.027, 0.032)	0.000 (0.000, 0.007)	0.155 (0.154, 0.156)
Different-Source	0.008 (0.007, 0.009)	0.007 (0.007, 0.008)	0.003 (0.002, 0.004)	0.104 (0.104, 0.104)
<i>damage excluded</i>	0.008 (0.006, 0.009)	0.006 (0.005, 0.006)	0.005 (0.005, 0.006)	0.087 (0.087, 0.087)
All Pairings	0.010 (0.009, 0.011)	0.013 (0.012, 0.013)	0.004 (0.003, 0.005)	0.115 (0.115, 0.115)
<i>damage excluded</i>	0.008 (0.007, 0.009)	0.015 (0.014, 0.016)	0.003 (0.000, 0.004)	0.103 (0.103, 0.103)

Table 4: Pairwise score R&R model estimates for summary quantities,  $\sigma_{\text{repeat}}$  and  $\sigma_{\text{reprod}}$ .

Model	$\sigma_{\text{repeat}}$	$\sigma_{\text{reprod}}$
Same-Source	0.159	0.065
<i>damage excluded</i>	0.155	0.064
Different-Source	0.104	0.022
<i>damage excluded</i>	0.087	0.021
All Pairings	0.115	0.039
<i>damage excluded</i>	0.103	0.037

## 5 Conclusions

Our approach to adapting the Gauge R&R framework to two complex data structures was focused on preserving the model assumptions and structure of traditional Gauge R&R mixed-effects models. Adapting data science problems which leverage complex data structures to fit the traditional Gauge R&R framework has several advantages, the first of which is the preservation of the data format and units. Interpretability of estimated variance components is immediate and does not require any additional transformation or maneuvering.

In addition, the framework provides us with a way to estimate quantities relevant to the measurement process we are working inside of. Summary values such as  $\sigma_{\text{repeat}}$  and  $\sigma_{\text{reprod}}$  provide insight about the overall reproducibility of the measurement process, while variance components for study factors provide detailed insight on sources of variability. In our study, the variance components associated with device and operator were much smaller than those associated with differences across parts and residual error, which provides assurance that a minimal amount of measurement variability is due to procedural or mechanical differences across operators and devices. We are able to immediately gain this insight after modeling because of the R&R framework.

Another advantage of leveraging the Gauge R&R framework is that it provides us with actionable items within a measurement process. Our results indicated that operator variability was larger for lands with one or more unsuitable LEAs, and was greatly reduced after removal of the offending LEAs from modeling. This insight about the measurement process informed a larger focus on unsuitable LEAs and damaged bullets in training materials and Standard Operating Procedures for microscope operators.

An extremely useful by-product to the study is that we have also established what levels of variability are typically observed when repeated scans are gathered by trained operators in our measurement process. These standards can be used to assess scanning consistency for trainees as well as identify LEAs with damage or low scan quality.

Our approach to signature modeling emphasized subsampling to remove dependence and comply with Gauge

R&R model independence assumptions. Taking this approach with similar data structures requires considering window sizes and carefully balancing data reduction with reducing dependency. Future work should include investigating the possibility of incorporating dependency into the model, perhaps by considering a small slice of signature data, such as twenty consecutive  $x_{Li}$  locations. We may still be slightly underestimating variability due to a small positive correlation that remained present in the data.

Our focus here is on a specific application to a forensic bullet matching data pipeline; however, similar approaches can be applied to other data science pipelines. These adaptations are most directly applicable to structured response data or pairwise comparisons applications. Paired data are a commonly considered structure in data science, and this approach could be very advantageous to analyzing sources of variability in a variety of paired comparison frameworks.

The study design and results presented here resulted in actionable items for the automated firearms analysis measurement process. It is our hope that similar approaches with analogous or new data structures can yield researchers in other application fields similar results and insights.

## Bibliography

Wei Chu, T. Song, J. Vorburger, J. Yen, S. Ballou, and B. Bacharach. Pilot study of automated bullet signature identification based on topography measurements and correlations. *Journal of Forensic Sciences*, 55(2):341–47, 2010.

Wei Chu, Robert M Thompson, John Song, and Theodore V Vorburger. Automatic identification of bullet signatures based on consecutive matching striae (cms) criteria. *Forensic Science International*, 231(1-3):137–41, 2013.

J. De Kinder and M. Bonifanti. Automated comparison of bullet striations based on 3d topography. *Forensic Science International*, 101:85–93, 1999.

David Donoho. 50 years of data science. *Journal of Computational and Graphical Statistics*, 26(4):745–766, 2017. doi: 10.1080/10618600.2017.1384734. URL <https://doi.org/10.1080/10618600.2017.1384734>.

James E. Hamby, David J. Brundage, and James W. Thorpe. The identification of bullets fired from 10 consecutively rifled 9mm ruger pistol barrels: A research project involving 507 participants from 20 countries. *AFTE Journal*, 41(2):99–110, 2009.

Eric Hare, Heike Hofmann, and Alicia Carriquiry. Automatic matching of bullet land impressions. *The Annals of Applied Statistics*, 11:2332–2356, 12 2017.

Douglas C. Montgomery and George C. Runger. Gauge capability analysis and designed experiments. part ii: Experimental design models and variance component estimation. *Quality Engineering*, 6(2):289–305, 1993. doi: 10.1080/08982119308918725. URL <https://doi.org/10.1080/08982119308918725>.

Rogerio Santana Peruchi, Pedro Paulo Balestrassi, Anderson Paulo de Paiva, Joao Roberto Ferreira, and Michele de Santana Carmelossi. A new multivariate gage r&r method for correlated characteristics. *International Journal of Production Economics*, 144(1):301 – 315, 2013. ISSN 0925-5273. doi: <https://doi.org/10.1016/j.ijpe.2013.02.018>. URL <http://www.sciencedirect.com/science/article/pii/S0925527313000856>.

Kiegan Rice, Ulrike Genschel, and Heike Hofmann. A robust approach to automatically locating grooves in 3d bullet land scans. *Journal of Forensic Sciences*, 65(3):775–783, 2020. doi: 10.1111/1556-4029.14263. URL <https://onlinelibrary.wiley.com/doi/abs/10.1111/1556-4029.14263>.

Shannon Sweeney. Analysis of two-dimensional gage repeatability and reproducibility. *Quality Engineering*, 19(1):29–37, 2007. doi: 10.1080/08982110601057641. URL <https://doi.org/10.1080/08982110601057641>.

Stephen B. Vardeman and Enid S. VanValkenburg. Two-way random-effects analyses and gauge r&r studies. *Technometrics*, 41(3):202–211, 1999. ISSN 00401706. URL <http://www.jstor.org/stable/1270565>.